

# Internal Energy Dissipators for Culverts on Steep Slopes with Inlet Control

A. L. SIMON, S. SARIKELLE, AND S. F. KOROM

Results of a model study of internal energy dissipators for culverts on a steep slope and operating under inlet control are discussed. The shortest ring chamber design that effectively reduces the outlet velocity is provided. Ring chamber diameters are expressed as a function of the upstream Froude number. Spacing and dimensions of roughness elements are related to ring chamber diameter. The model results are compared with prototype performance and adjusted to improve their accuracy. Hydraulic design parameters that affect the operation of such culverts are discussed, and practical design procedures are given.

Because a culvert offers less resistance to flow than does a natural stream channel, water usually exits a culvert with greater velocity. This increase in velocity can cause excessive erosion or scour of the downstream channel and lead to structural failure of the highway embankment and the culvert itself. For low outlet velocities, lining the downstream channel with rocks offers sufficient protection against erosion and scour. Rock protection is not sufficient, however, for high outlet velocities. For example, the Ohio Department of Transportation's (ODOT's) design manual specifies that rock channel protection should not be used for outlet velocities greater than 20 ft/sec (1). These higher velocities are often reduced by the formation of a hydraulic jump that produces an outlet flow of greater depth and lower velocity. The hydraulic jump is usually produced by an energy dissipator constructed at the outlet of the culvert; but, if the culvert is on a steep slope and under inlet control (i.e., a high-energy culvert), a hydraulic jump can be formed in the culvert itself. This allows the energy dissipator at the culvert's exit to be simplified or even eliminated.

Hydraulic jumps in culverts can be produced by placing rings (roughness elements) on the inside perimeter of the culvert near the outlet. This end section with rings in it is set on a milder slope than the rest of the culvert and is called a ring chamber. Summarized here are the results of an ODOT-sponsored study (2) undertaken to develop the hydraulic design parameters necessary to optimize the design of ring chambers that effectively reduce the outlet velocities of high-energy culverts by producing a hydraulic jump in the ring chamber.

Department of Civil Engineering, The University of Akron, Akron, Ohio 44325.

## BACKGROUND

### Development of Ring Chamber

The use of circular roughness elements in high-energy culverts was first studied by Wiggert and Erfle (3) and Wiggert et al. (4). They placed circular rings inside the periphery of model culverts of constant slope. For the culvert to flow full at the location of the dissipators, four dissipators of two different heights were needed. A larger ring upstream created a hydraulic jump that was maintained by three smaller rings downstream. The upstream ring was approximately twice the height of the downstream rings and was spaced approximately twice as far from them as they were from each other. These findings led to sizing and locating the downstream rings as dictated by the following equations:

$$0.06 \leq K/D \leq 0.09 \quad (1)$$

and

$$L/D = 1.5 \quad (2)$$

where

- $K$  = the height of the dissipators (ft),
- $D$  = the inside diameter of the culvert (ft), and
- $L$  = the spacing between the three smaller rings (ft).

Wiggert et al. also found that by maintaining a free surface throughout the length of a culvert with rings in it, a greater velocity reduction could be achieved than under full-flow conditions. This introduced the telescoping ring chamber in which the main section (inlet section) of the culvert is governed by the conventional design parameters and the ring chamber is sized by the following equation:

$$(Q^2/0.10g)^{1/5} < D_o < (Q^2/0.044g)^{1/5} \quad (3)$$

where

- $Q$  = the design flow (ft<sup>3</sup>/sec),
- $g$  = the acceleration due to gravity (ft<sup>3</sup>/sec), and
- $D_o$  = the inside diameter of the ring chamber (ft).

Equation 3 requires five rings sized and spaced according to

$$0.10 \leq K/D_o \leq 0.15 \quad (4)$$

and

$$1.5 \leq L/D_o \leq 2.5 \quad (5)$$

This free-surface design produced a tumbling flow characterized by acceleration between rings and a hydraulic jump over each ring. This produced velocity reductions ranging from 50 to 70 percent.

ODOT designed their first ring chamber for a high-energy culvert in 1974 using the equations for free-surface flow. The culvert and ring chamber were placed on a 4.4 percent slope. Pettit (5) suggested the need to reduce the slope of the ring chamber to 0.5 percent and add a settling distance beyond the last ring station. The steep 4.4 percent slope established a vertical velocity component that produced a scour hole at the outlet of the ring chamber. The settling distance allows the flow held back by the last dissipator to tumble to a lesser depth within the confines of the culvert. All subsequent ODOT high-energy culvert designs have ring chambers set at a slope of 0.5 percent or less.

ODOT also modified the shape of the dissipators from a solid ring to two ring segments (Figure 1). If water trapped in

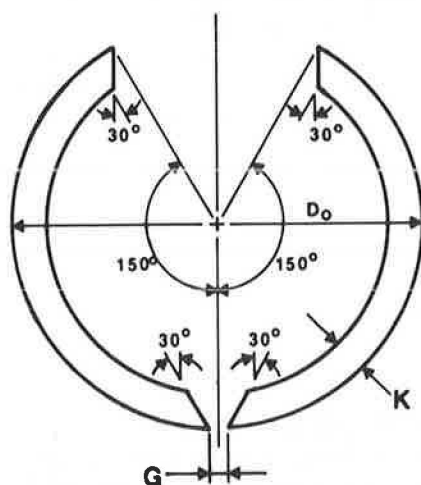


FIGURE 1 Modified two-piece dissipator.

front of the solid rings froze, it could damage the joint between the dissipators and the inner wall of the ring chamber. The gap ( $G$ ) was added at the bottom to allow for complete drainage. Removal of a section of the ring at the top promotes free-surface flow throughout the culvert. The upstream edge of the

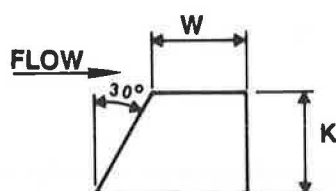


FIGURE 2 Cross section of ODOT dissipators.

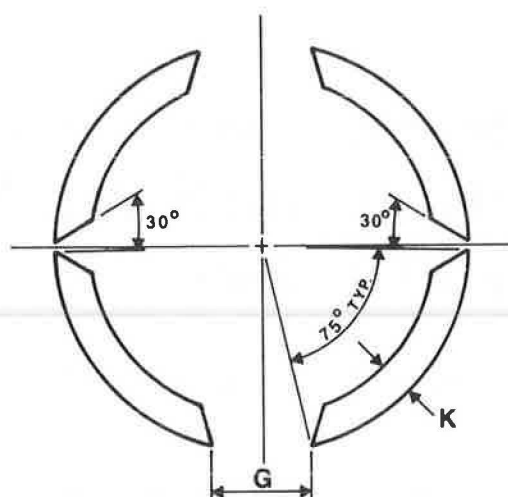


FIGURE 3 Four-piece dissipator.

rings also had a 30-degree bevel added to aid in passing debris (Figure 2). All of these changes were substantiated in laboratory and field tests by Simon and Sarikelle (6).

ODOT later modified the ring dissipators from a two-piece to a four-piece design to simplify their installation in the ring chamber (Figure 3).

### Froude Numbers Used in the Study

Because the dominant forces in open channel problems are controlled by gravity, viscous and other effects can be neglected and Froude modeling law will apply. This means that the ratio of gravitational forces to inertial forces will be the same in both model and prototype to maintain dynamic similarity. The Froude number is given by

$$F = V/(gL')^{1/2} \quad (6)$$

where  $V$  is the velocity of the flow and  $L'$  is a characteristic length, which for open-channel flow is the hydraulic depth. This value is defined as the area of flow normal to the flow's direction divided by the top width of the free surface. For rectangular channels this is simply the depth of flow. For circular channels, hydraulic depth computations are more complex. To simplify Froude number computations for circular channels in this study the hydraulic depth has been replaced by the actual depth.

Alternately, the true Froude number for a circular channel flowing less than half full can be approximated using

$$F' = 1.135F^{1.019} \quad (7)$$

where  $F'$  is the true Froude number computed using the hydraulic depth and  $F$  is the Froude number computed using the actual depth.

### EXPERIMENTAL PROCEDURE

Models of culverts similar to the one shown in Figure 4 were assembled of clear acrylic in an adjustable-slope flume so that

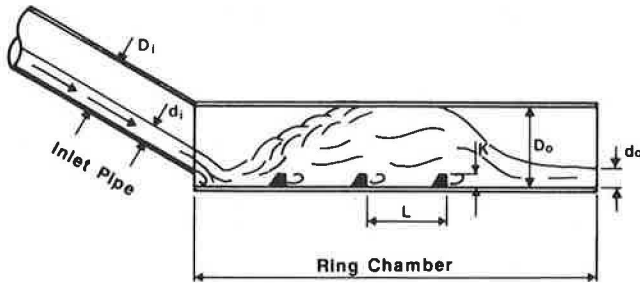


FIGURE 4 Ring chamber flowing just full.

ring dissipators of various numbers, types, and heights ( $K$ ) could be used, distances between dissipators ( $L$ ) could be varied, and the slope of the inlet pipe could be changed.

The ring chamber had an inside diameter ( $D_o$ ) of 6.0 in. Four inlet pipes were used with inside diameters ( $D_i$ ) of 4.0, 4.75, 5.5, and 6.0 in. This gave ring chamber-to-inlet size ratios ( $D_o/D_i$ ) of 1.50, 1.26, 1.09, and 1.00, respectively.

Ring dissipators were molded to model the four-piece design shown in Figure 3 and a new two-piece design shown in Figure 5. This new design is the same as the four-piece design with the top two ring segments eliminated. It was believed that only the two bottom segments were necessary to produce a hydraulic jump in the ring chamber. Both designs were molded with dissipator heights ( $K$ ) of 0.50, 0.75, and 1.00 in. to give relative heights ( $K/D$ ) of  $1/12$ ,  $1/8$ , and  $1/6$ , respectively.

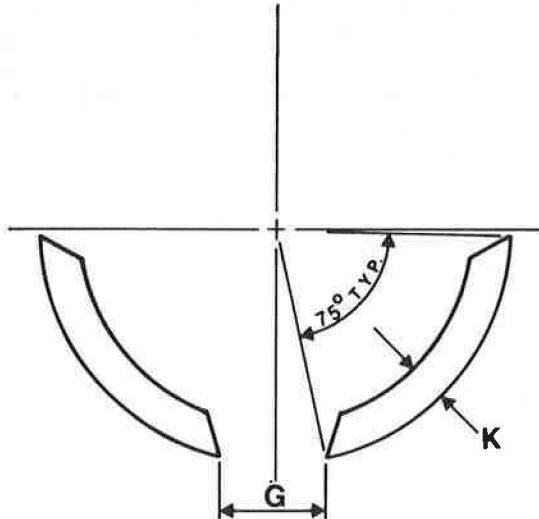


FIGURE 5 Improved two-piece dissipator.

Holes were drilled in the inlet pipes and ring chamber so flow depths could be measured with a point gauge. When these depths and the amount of flow ( $Q$ ) from a calibrated flowmeter are known, the velocities can be computed.

Tests were run to find the minimum number of dissipators, the type of dissipators, the minimum relative height of dissipators ( $K/D_o$ ), and the minimum relative spacing between dissipators ( $L/D_o$ ) that produced a hydraulic jump in the ring chamber. It was found that four two-piece dissipators (as in Figure 5) with  $K/D_o$  of  $1/8$  and  $L/D_o$  of 1.0 produced one minimum design. Another was three two-piece dissipators with

$K/D_o$  of  $1/6$  and  $L/D_o$  of 1.0. Other designs worked as well but required longer ring chambers or larger ring chamber diameters for a given inlet pipe size and design flow.

To test the design of four two-piece dissipators with  $K/D_o$  of  $1/8$  and  $L/D_o$  of 1.0, the inlet pipe was placed on a slope of approximately 2 to 1. The discharge was increased until the ring chamber flowed just full (Figure 4), and the inlet and outlet flow depths were measured ( $d_i$  and  $d_o$ , respectively). The inlet flow depth was measured one ring chamber distance from the end of the inlet pipe. Next, the discharge was increased until a full-flow condition developed in the inlet pipe to a one ring chamber diameter distance into the pipe (Figure 6). (This was not done for  $D_o/D_i = 1.50$ ). This is called a choked condition. The values for  $d_i$  and  $d_o$  were measured again. These steps were repeated for decreasing values of the inlet pipe's slope. The procedure was followed for each of four inlet pipe diameters: 4.00, 4.75, 5.5, and 6.00 in.

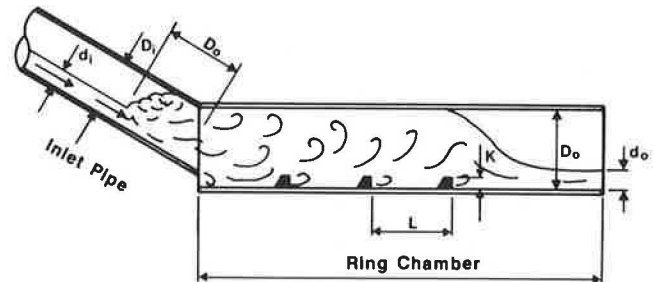


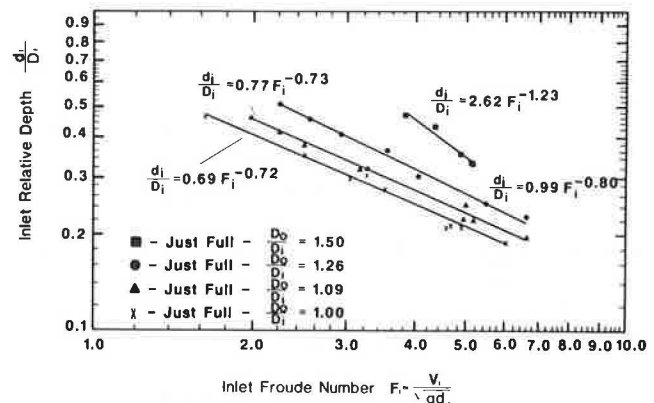
FIGURE 6 Ring chamber flowing fully choked.

To test the design of three two-piece dissipators with  $K/D_o$  of  $1/6$  and  $L/D_o$  of 1.0, the procedure was repeated, but measurements were taken only for choked conditions.

All of the tests were carried out with the ring chamber set at a slope of 0.5 percent.

## DISCUSSION OF RESULTS

This section has two parts. In the first are discussed the results shown in Figures 7–10, which represent the results obtained from the model studies. The second part covers two studies comparing the energy reduction performance of models and

FIGURE 7 Performance graph for just-full conditions: four dissipators ( $K/D_o = 1/8$ ,  $L/D_o = 1.0$ ).

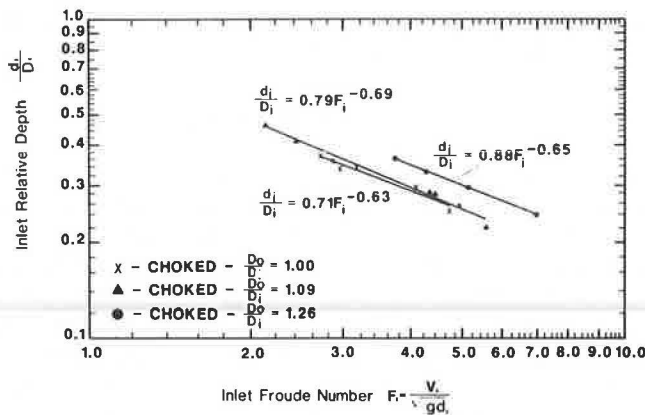


FIGURE 8 Performance graph for choked conditions: four dissipators ( $K/D_o = 1/8$ ,  $L/D_o = 1.0$ ).

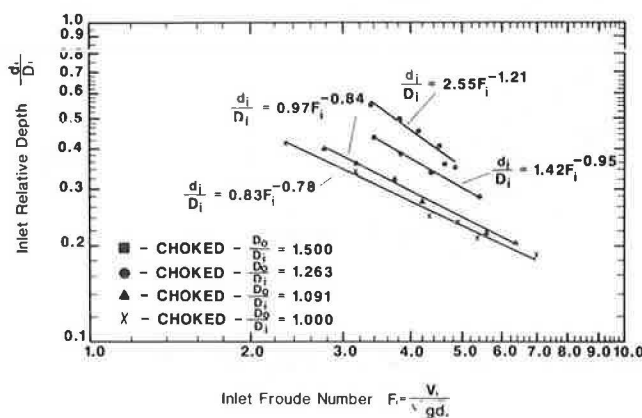


FIGURE 9 Performance graph for choked conditions: three dissipators ( $K/D_o = 1/6$ ,  $L/D_o = 1.0$ ).

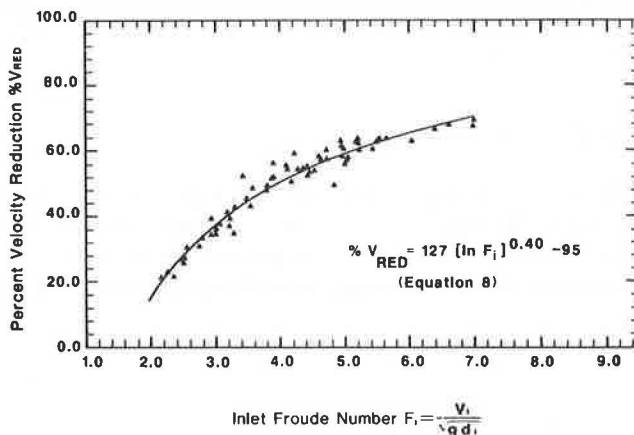


FIGURE 10 Best-fit curve for percent velocity reduction.

prototypes of high-energy culverts with ring chambers. This information is used to calibrate the velocity reduction curve shown in Figure 10, which can be used to predict velocity reductions in prototype applications.

### Graphic Presentation of Results

Figures 7–9 show the inlet Froude number ( $F_i$ ) and the inlet relative depth ( $d_i/D_i$ ) necessary to cause certain flow conditions in the ring chamber. For instance, in Figure 7 the bottom line

represents the best fit through data points taken from tests of four two-piece dissipators where  $K/D_o = 1/8$ ,  $L/D_o = 1.0$ , the ring chamber diameter was the same as the inlet pipe diameter ( $D_o/D_i = 1.00$ ), and the culvert was flowing just full. Points on this line give the inlet Froude number and inlet relative depth necessary to cause the given ring chamber to flow just full (Figure 4). Points below this line indicate less than full flow condition for the given Froude number and inlet relative depth. Similarly, any point above this line indicates a pressurized flow condition for the Froude number and inlet relative depth given.

The next line gives the inlet Froude numbers and inlet relative depths for just-full conditions when the ring chamber diameter is 1.09 times larger than the inlet pipe diameter.

The difference between Figures 7 and 8 is that the latter represents choked conditions (Figure 6).

Figure 9 is also for choked conditions but with a shorter ring chamber with fewer but larger dissipators (i.e., three two-piece dissipators with  $K/D_o = 1/6$  and  $L/D_o = 1.0$ ).

Figure 10 shows percent velocity reduction ( $\%V_{RED}$ ) as a function of  $F_i$ . Inlet relative depth values from all three sets of tests are represented. The best-fit equation for percent velocity reduction is

$$\%V_{RED} = 127 [\ln(F_i)]^{0.40} - 95 \quad (8)$$

where  $\ln(F_i)$  indicates the natural logarithm of the inlet Froude number.

The limited amount of scatter about the best-fit curve shown in Figure 10 suggests that all of the ring chamber designs tested caused about the same velocity reduction for a given inlet Froude number. This implies that the hydraulic jump causes the velocity reduction (i.e., the design of the ring chamber that produces the jump is relatively insignificant). Thus the ring chamber design that produces hydraulic jumps and is most economical to construct may be selected without limiting velocity-reducing capacity.

A similar figure showing percent energy reduction ( $\%E_{RED}$ ) as a function of  $F_i$  could also be drawn. The best-fit equation for percent energy reduction for all tests is

$$\%E_{RED} = 160 [\ln(F_i)]^{0.35} - 115 \quad (9)$$

### Prototype Ring Chamber Tests and Calibration of Velocity Reduction Curve

Wiggert et al. (4) compare energy reductions in a 6-in.-diameter model and an 18-in.-diameter concrete prototype. Simon and Sarikelle (6) compare results for a model with a 4.06-in. inlet and a 5.69-in. ring chamber with those for a concrete prototype with a 60-in. inlet and an 84-in. ring chamber. Both sets of results are given in Table 1.

The differences in energy reductions between the models and prototypes are mainly due to viscous shear forces. Although these forces are not as significant as gravitational forces, in open-channel flow they affect the results. Viscous effects in prototype scale are not necessarily the same as those in the corresponding models that were built according to Froude's law. Comparison of model and field studies has shown that viscous forces affect the flow more in a smaller-diameter pipe than in a larger-diameter pipe. Energy losses in the smaller models should be greater than energy losses in the

TABLE 1 COMPARISON OF MODEL AND PROTOTYPE ENERGY REDUCTIONS

| Model Diameter, $D_o$ (in.) | Prototype Diameter, $D_o$ (in.) | Model Energy Reduction (%) | Prototype Energy Reduction (%) | Difference in Energy Reduction (%) |
|-----------------------------|---------------------------------|----------------------------|--------------------------------|------------------------------------|
| 6                           | 18                              | 87.2                       | 65.0                           | 25.5                               |
| 6                           | 18                              | 83.6                       | 53.0                           | 36.6                               |
| 6                           | 84                              | 90.0 <sup>a</sup>          | 55.8                           | 38.0                               |
| 6                           | 84                              | 90.0 <sup>a</sup>          | 60.2                           | 33.1                               |

<sup>a</sup>Estimated value based on results in Simon and Sarikelle (6).

larger prototypes. These results are given in Table 1. The values in the last column of this table show that the energy-reducing performance of the prototypes is approximately one-third less than predicted by the models. This rather significant difference may be explained by the fundamental laws of hydraulic modeling. Expressing the ratio of viscous forces per unit discharge, it is found that it equals the square root of the length ratio of the model to the prototype (7). Consequently, a culvert that is nine times larger than the model would have one-third of the viscous force per unit discharge of the model. Because energy losses are proportional to the viscous shear in the fluid, it is explainable that there is relatively more energy lost per unit volume flowing in the model. For this reason, the energy reduction equation for the models in this study (Equation 9) can be reduced one-third. It becomes

$$\%E_{RED} = 107 [\ln(F_i)]^{0.35} - 77 \quad (10)$$

Computations show that if the energy reduction equation is reduced by one-third, the velocity reduction equation should also be reduced. But the amount of this reduction varies depending on the inlet pipe's flow conditions ( $F_i$  and  $d_i/D_i$ ). Because of this and in recognition of the limited amount of prototype performance data available for this study, it is recommended that the velocity reduction equation also be reduced one-third. It becomes

$$\%V_{RED} = 85 [\ln(F_i)]^{0.40} - 63 \quad (11)$$

Figure 11 shows a plot of Equation 11. It should only be used for culverts 18 in. or larger in diameter.

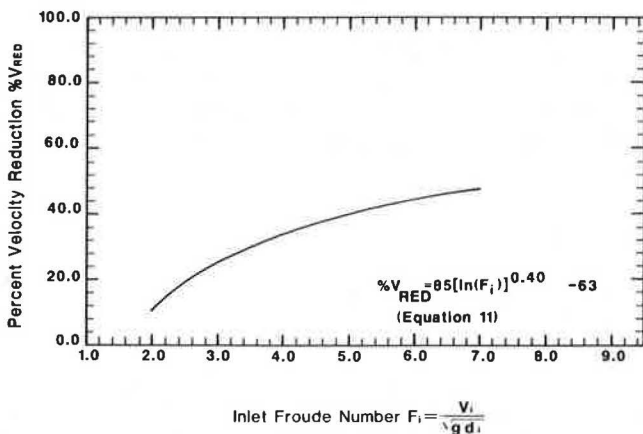


FIGURE 11 Calibrated percent velocity reduction curve for prototypes.

## CONCLUSIONS

Close inspection of the results shown in Figures 7–9 reveals that of the three sets of tests the two for choked conditions allow for higher Froude numbers and inlet relative depths for a given  $D_o/D_i$ -value. Therefore the design flow can be greater for given diameters of the inlet and ring chamber if the ring chamber is designed to flow fully choked rather than just full. There is not a large difference between the results for the two sets with choked conditions so it is better to use the ring chamber design that would be less expensive to construct. Therefore the design with three two-piece dissipators (Figure 5) with  $K/D_o = 1/6$  and  $L/D_o = 1.0$  should be chosen over the design with four two-piece dissipators with  $K/D_o = 1/8$  and  $L/D_o = 1.0$  because it allows for a shorter ring chamber. This design follows the data shown in Figure 9.

Figure 12 is a reproduction of Figure 9 that may be used as a design aid for determining choked-flow conditions in ring chambers of various sizes. Designs with inlet relative depths and inlet Froude numbers that fall on or below the appropriate values are acceptable.

Other hydraulic design parameters that affect the operation of a ring chamber are discussed next.

### Slope

Results shown in Figures 7–9 were obtained with the ring chamber set at a 0.5 percent slope. Slight variations from this slope did not affect the performance of the ring chamber. It is therefore recommended that the slope be kept in the range of 0.2 to 0.7 percent.

### Distance to First Dissipator

The distance from the end of the inlet pipe to the first dissipator ( $L_1$ ) should be set at  $1.33 D_o$ . If it is less than this value and the inlet pipe–ring chamber connection is built such that there is a drop from the invert of the inlet to the invert of the ring chamber, the flow could shoot over the first dissipator.

### Drainage Gap

The drainage gap ( $G$ ) between the two segments that make up each dissipator was sized by ODOT (Pettit, unpublished data) to be in the range:

$$1/13 \leq G/D_o \leq 1/6.5 \quad (12)$$

In this study,  $G/D_o = 1/8$ ; therefore it is recommended that

$$1/13 \leq G/D_o \leq 1/8 \quad (13)$$

### Dissipator Width

The dissipator width ( $W$ ) is based on structural considerations. It should be wide enough to allow reinforcing bars to be placed in the dissipator segments to protect them from damage from collisions with passing debris. The dissipator widths given in Table 2 are those given by ODOT (Pettit, unpublished data).



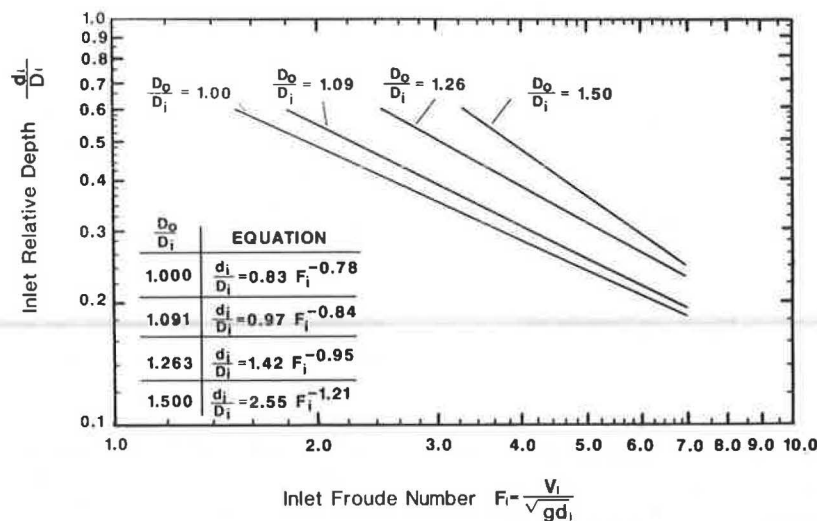
FIGURE 12 Design graph for ring chamber diameter sizes ( $D_o$ ).

TABLE 2 RING CHAMBER DESIGN GUIDE

| $D_o$<br>(in.) | $D_o$<br>(ft.) | $L_1$<br>(ft.) | $L$<br>(ft.) | $L_s$<br>(ft.) | $L_o$<br>(ft.) | $K$<br>(in.) | $G$<br>(in.) | $W$<br>(in.) |
|----------------|----------------|----------------|--------------|----------------|----------------|--------------|--------------|--------------|
| 36             | 3              | 4              | 3            | 6              | 16             | 6            | 4            | 7            |
| 42             | 3-1/2          | 6              | 4-1/2        | 9              | 24             | 7            | 5            | 7            |
| 48             | 4              | 6              | 4-1/2        | 9              | 24             | 8            | 6            | 8            |
| 54             | 4-1/2          | 6              | 4-1/2        | 9              | 24             | 9            | 6            | 8            |
| 60             | 5              | 8              | 6            | 12             | 32             | 10           | 7            | 9            |
| 66             | 5-1/2          | 8              | 6            | 12             | 32             | 11           | 8            | 9            |
| 72             | 6              | 8              | 6            | 12             | 32             | 12           | 9            | 9            |
| 78             | 6-1/2          | 10             | 7-1/2        | 15             | 40             | 13           | 9            | 9            |
| 84             | 7              | 10             | 7-1/2        | 15             | 40             | 14           | 10           | 9            |
| 90             | 7-1/2          | 10             | 7-1/2        | 15             | 40             | 15           | 11           | 9            |
| 96             | 8              | 12             | 9            | 18             | 48             | 16           | 12           | 10           |
| 102            | 8-1/2          | 12             | 9            | 18             | 48             | 17           | 12           | 10           |
| 108            | 9              | 12             | 9            | 18             | 48             | 18           | 13           | 10           |
| 114            | 9-1/2          | 14             | 10-1/2       | 21             | 56             | 19           | 14           | 10           |
| 120            | 10             | 14             | 10-1/2       | 21             | 56             | 20           | 15           | 10           |
| 126            | 10-1/2         | 14             | 10-1/2       | 21             | 56             | 21           | 15           | 12           |
| 132            | 11             | 16             | 12           | 24             | 64             | 22           | 16           | 12           |
| 138            | 11-1/2         | 16             | 12           | 24             | 64             | 23           | 17           | 12           |
| 144            | 12             | 16             | 12           | 24             | 64             | 24           | 18           | 12           |
| 150            | 12-1/2         | 18             | 13-1/2       | 27             | 72             | 25           | 18           | 12           |
| 156            | 13             | 18             | 13-1/2       | 27             | 72             | 26           | 19           | 12           |
| 162            | 13-1/2         | 18             | 13-1/2       | 27             | 72             | 27           | 20           | 15           |
| 168            | 14             | 20             | 15           | 30             | 80             | 28           | 21           | 15           |
| 174            | 14-1/2         | 20             | 15           | 30             | 80             | 29           | 21           | 15           |
| 180            | 15             | 20             | 15           | 30             | 80             | 30           | 22           | 15           |

### Settling Distance

The settling distance ( $L_s$ ) is the distance from the last dissipator to the end of the ring chamber. In this region water obstructed by the last dissipator tumbles to a lesser depth. The settling distance should be long enough to contain this tumbling action

so that it does not increase the erosion potential at the culvert's exit. This acceleration to a lesser depth is completed within a  $2D_o$  distance after the last dissipator.

### Tailwater Effects

The results in this study were obtained with no tailwater. If a prototype has tailwater sufficient to maintain subcritical flow, it will tend to further reduce the outlet velocity; however, it is noted that for most inlet-control conditions tailwater is not considered effective in reducing outlet velocities (8). Excessive tailwater above the culvert outlet concentrates flow. Tailwater conditions also affect the geometry of the scour hole. The reader should check a study of this subject conducted by the U.S. Army Corps of Engineers (9).

### Venting

When a hydraulic jump is produced in the ring chamber it can cause a negative pressure in the inlet. This negative pressure can be eliminated by venting the pipe anywhere upstream of the hydraulic jump. It is known that venting causes the exit velocity to increase, but the amount of increase cannot be measured accurately because of air entrainment in the outlet flow.

If venting is desired, the diameter of the ring chamber should be increased to the next available pipe size over the one determined by the design procedure described hereafter. (Other hydraulic parameters should increase for the new  $D_o$  as in Table 2).

### Design Procedure

The steps necessary to design a ring chamber based on the results of this study follow.

1. Find outlet velocity: The flow in most properly vented culverts on steep slopes reaches normal depth by the end of the culvert (9). Compute the outlet velocity based on normal depth of the culvert without a ring chamber on it. This step can be

simplified by using information such as that given in Hydraulic Design Series 3 (10).

If the computed velocity exceeds the maximum allowable for rock channel protection [20 ft/sec for ODOT (1)] and the culvert is on a steep slope and under inlet control, a ring chamber based on this study can be used to reduce outlet velocity.

2. Assume ring chamber diameter size ( $D_o$ ): Assume a ring chamber-to-inlet ratio ( $D_o/d_i$ ). To start with, choose a diameter of ring chamber from commercially available culvert sizes such that  $D_o/d_i$  is close to 1.25. The length of the ring chamber ( $L_o$ ) is then obtained from Table 2.

3. Find new slope of inlet pipe: Find the new slope of the inlet pipe now that a ring chamber with a slope of from 0.2 to 0.7 percent is to be attached to it. This involves some simple trigonometry.

4. Find new inlet velocity and normal depth: Find, at the end of the inlet, the new velocity as in Step 1 and the normal depth, both with the new slope found in Step 3.

5. Check Figure 12: Find  $F_i$  at the end of the inlet using the normal depth from Step 4 and check Figure 12 to see if the assumed ring chamber size is correct. If it is not, repeat Steps 2 through 4 with increasingly larger or smaller ring chamber diameters until the results agree with Figure 12.

For  $D_o/d_i$ -values not represented by the equations on Figure 12, it is necessary to linearly interpolate between the two closest lines that are represented by equations. For instance, if  $D_o/d_i = 1.4$ , it is necessary to linearly interpolate between the lines for  $D_o/d_i = 1.26$  and  $D_o/d_i = 1.50$ .

6. Find reduced outlet velocity: Find the reduced outlet velocity with Equation 11 or Figure 11. If the outlet velocity is still greater than the maximum allowable for rock channel protection, additional measures will be needed to reduce this velocity.

7. Check if venting is necessary: If venting is necessary, the diameter of the ring chamber should be increased to the next available size greater than that found in Step 5.

8. Find other hydraulic parameters: With the  $D_o$  found in Step 5 or 7, determine  $L_1$ ,  $L$ ,  $L_s$ ,  $L_o$  (total length of ring chamber),  $K$ ,  $G$ , and  $W$  from Table 2.

## ACKNOWLEDGMENTS

The authors are indebted to the Ohio Department of Transportation for its continued support of their research on energy dissipation in culverts. The success of this study was greatly enhanced by the helpful advice of John D. Herl, John O. Hurd, C. Gene Pettit, and Leon O. Talbert of ODOT. Also, the cooperation of the FHWA, U.S. Department of Transportation, is gratefully acknowledged along with the helpful comments of Marvin I. Espeland and his staff at FHWA.

## REFERENCES

1. *Location and Design Manual*. Ohio Department of Transportation, Columbus, Feb 1978, Section 1122.
2. A. L. Simon and S. Sarikelle. *Internal Energy Dissipators for Culverts*. Report FHWA/OH-84/007. Department of Civil Engineering, University of Akron, Akron, Ohio, Sept. 1984.
3. J. M. Wiggert and P. D. Erfle. Culvert Velocity Reduction by Internal Energy Dissipators. *Concrete Pipe News*, American Concrete Pipe Association, Arlington, Va., Oct. 1972, pp. 87-93.
4. J. M. Wiggert, P. D. Erfle, and H. M. Morris. Roughness Elements as Energy Dissipators of Free-Surface Flow in Circular Pipes. In *Highway Research Record 373*, HRB, National Research Council, Washington, D.C., 1971, pp. 64-73.
5. C. G. Pettit. The Enclosure of Permars Run. *Concrete Pipe News*, American Concrete Pipe Association, Arlington, Va. Feb. 1980, pp. 7-11.
6. A. L. Simon and S. Sarikelle. *Field and Laboratory Evaluation of Energy Dissipators for Culverts and Storm Drain Outlets*. Report Ohio DOT-03-79. Department of Civil Engineering, University of Akron, Akron, Ohio, Dec. 1980, Vol. 1, pp. 87-90.
7. A. L. Simon. *Hydraulics*, 3rd ed. John Wiley and Sons, New York, 1986.
8. Hydraulic Charts for the Selection of Highway Culverts. In *Hydraulic Engineering Circular 5*, Office of Engineering, FHWA, U.S. Department of Transportation, Dec. 1965, Chapter II, pp. 5-12.
9. Hydraulic Design of Energy Dissipators for Culverts and Channels. In *Hydraulic Engineering Circular 14*, Office of Engineering, FHWA, U.S. Department of Transportation, Nov. 1975, Chapters 3 and 5, pp. III-3 and V-1 to V-6.
10. *Design Charts for Open-Channel Flow*. Hydraulic Design Series 3. FHWA, U.S. Department of Transportation, March 1979.